Available online at www.sciencedirect.com
SCIENCE DIRECT®
Thermochimica Acta 403 (2003) 55–63
thermochimica acta
www.elsevier.com/locate/tca

Scanning microcalorimetry at high cooling rate

S.A. Adamovsky [a], A.A. Minakov [b], C. Schick [a,*]

[a] *Department of Physics, University of Rostock, Universitaetsplatz 3, 18051 Rostock, Germany*
[b] *Natural Science Center of General Physics Institute, Vavilov st. 38, 199911 Moscow, Russia*

Received 20 November 2002; received in revised form 5 March 2003; accepted 17 March 2003

Abstract

Heat capacity measurements at fast cooling and heating were realized for linear polyethylene NBS SRM (standard reference material) 1484 sample, ca. 120 ng, in the melting-crystallization region. A commercial vacuum sensor, thermal conductivity gauge TCG-3880, Xensor Integrations, was utilized as a cell for a micro-calorimeter suitable for such measurements. The cell consists of a thin-film Si_3N_x membrane with a film-thermopile and a film-heater, which are formed at the membrane center. The current at the heater as well as the signal from the thermopile were monitored in real time during fast scanning of temperature of the central part of the membrane. The measurements were performed in an ambient gas, so that controlled cooling and heating rates up to 5×10^3 K/s were achieved. As conditions were not adiabatic, the heat leakage from the sample was calibrated and was taken into account for heat capacity measurements. A simple calibration algorithm was developed for such measurements. Thus, a step towards ultra fast cooling scanning calorimetry was made.

Keywords: Ultra fast scanning calorimetry; Scanning microcalorimetry; Melting and crystallization

1. Introduction

The interest in ultra fast scanning calorimetry is at least due to three reasons.

(i) Most of the modern materials are used in non-equilibrium states. To study the actual thermodynamic state of such materials at room temperature, e.g. of a semicrystalline polymer, requires high heating rates to prevent reorganization during the scan. These non-equilibrium states are generated by rapid cooling during processing of the material. Therefore, calorimetric experiments at cooling rates comparable to that during injection molding, as an example, are needed to study phase transitions under realistic processing conditions. With common DSC apparatuses, like the Perkin-Elmer Instruments Pyris DSC, calorimetric measurements at constant cooling rates up to 500 K/min (ca. 10 K/s) can be realized as shown recently by Mathot and co-workers [1]. Even though Mathot gives interesting results, he uses a cooling rate, which is far too slow to mimic realistic cooling conditions at injection molding of thin wall products which may reach hundreds or even thousands of kelvin per second [2–4].
(ii) Currently material science focuses on nano-scale systems. It is very difficult to perform calorimetric measurements of nano-gram samples, like thin films, because the heat flow needed to heat the sample at moderate rates is extremely small

* Corresponding author. Tel.: +49-381-4986880; Fax: +49-381-4981644.
E-mail address: christoph.schick@physik.uni-rostock.de (C. Schick).

0040-6031/03/$ – see front matter © 2003 Elsevier Science B.V. All rights reserved.
doi:10.1016/S0040-6031(03)00182-5

(ca. 0.3 nW at 10 K/min for 20 mm^2 of a 100 nm thick film) and cannot be detected by conventional calorimeters. In order to overcome the limitations heating rates can be increased inversely proportional to sample mass yielding heat flows which can be detected by ultra light calorimetric sensors as shown by Allen and co-workers [5–8].

(iii) The combination of high heating and cooling rates with small sub milligram sample masses opens up the application of calorimetry for high throughput analysis as needed for combinatorial chemistry [9].

To perform calorimetry at high rates sample and addenda should have sufficiently small heat capacity, e.g. below μJ/K. Such calorimeters were realized as thin film calorimeters which were first used in ac mode [10,11]. Also these calorimeters are able to heat and cool very fast by applying a high frequency current (several hundreds Hz) to the heater they were never used for fast cooling scans over a large temperature range by utilizing the heater on the membrane. Quasi-adiabatic scanning calorimetry at high heating rates, ca. 500 K/s, was developed by Hager [12] and even for rates up to 10^5 K/s, by Allen and co-workers [5–8].

Ultra fast scanning calorimetry provides important information on thermodynamic properties and structure changes in materials at high-speed thermal treatments, as well as on size-dependent effects in thin films and nanoparticles [5,6]. Allen and co-workers recently developed a thin-film differential scanning calorimetry (TDSC) for ultra fast heating [7]. The cell of the calorimeter consists of a thin film-heater, Ni or Pt ca. 50 nm, which was deposited on a thin, ca. 30 nm, Si_3N_x membrane. The heater simultaneously serves as a resistive thermometer. Thus, the heat capacity of discontinuous metal films [5,6] and separated polymer crystals [8] at ultrafast heating, ca. 10^5 K/s, can be investigated. Near-adiabatic conditions were achieved, when the cell was placed in vacuum ca. 10^{-5} to 10^{-6} Pa. Because the heater is simultaneously used as the temperature sensor, calorimetry during cooling may be difficult [13].

The possibility of heat capacity measurements at high cooling rates is also important for investigation of crystallization and amorphyzation processes at quenching. The heating rate can be enlarged by increasing heating power and decreasing mass of the measuring cell and the sample [5–8,12,14]. On the other hand, the only way to increase cooling rate up to 10^3 K/s and larger is diminishing of the cell-sample thickness, since the cooling possibility of any system is restricted by a finite heat transfer from the sample. The heat transfer is limited by the thermal conductivity of a cooling agent. In this case the measurements are non-adiabatic.

In this paper we focus on fast cooling scanning calorimetry using thin film sensors as proposed in [15,16]. The aim of the present work is to do a step towards ultra fast cooling scanning calorimetry which was, to the best of our knowledge, not realized before. A commercial thin film vacuum sensor, thermal conductivity gauge TCG-3880, Xensor Integrations, The Netherlands [17], was utilized as a calorimeter cell suitable for such measurements. The cell consists of a thin-film Si_3N_x membrane with a film-thermopile and a film-heater, which are placed at the center of the membrane. A linear polyethylene NBS SRM 1484 sample, ca. 120 ng, was placed at the center of the membrane just at the heater. The measurements were performed in an ambient gas, so that a relatively high cooling rate, ca. 5×10^3 K/s, was achieved for this sample. The conditions were non-adiabatic. The heat leakage from the sample was calibrated and was taken into account for the heat capacity measurements.

2. Method: measuring cell and calibration

The thermal conductivity gauge, TCG-3880, see [17] for details, consists of a ca. 500 nm thick Si_3N_x membrane with a semiconductive film-thermopile and a semiconductive resistive film-heater, ca. 50 μm × 100 μm, placed at the center of the membrane. The thermopile hot junctions are arranged around the heater at a distance ca. 40 μm from the center of the heater. The cold junctions are placed at the periphery of the cell, ca. 1 mm from the center, where the membrane is attached to the holder. Thus, the cold-junction temperature is the temperature of the holder and it is close to the temperature of the thermostat. An additional copper–constantan thermocouple was utilized for the measurement of the holder temperature, which was used as the reference temperature T_0. Such a cell with a sample is schematically shown in Fig. 1.

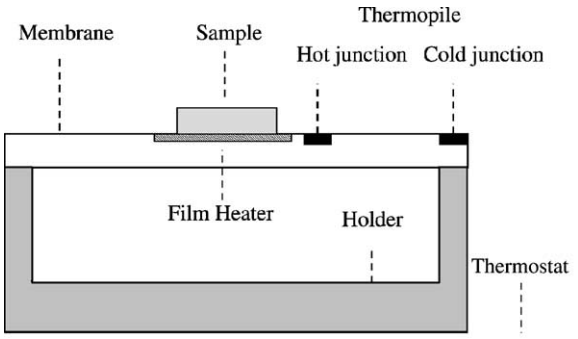

Fig. 1. Scheme of the experiment. The sample is placed at a flat thin membrane with a film-heater and a film-thermopile sensor. The cell is placed in a thermostat. The distance from membrane to thermostat wall is ca. 1 cm and from membrane to holder ca. 1 mm.

To allow fast cooling the cell is operated in an ambient gas. The heat transfer from the heated area to the environment can be described by a heat exchange parameter ξ measured in W/K. From the calibration curve of the TCG-3880 [17] it follows that at pressures below 0.1 Pa, when only heat transfer through the membrane exists, the gauge output voltage is 10 times larger than the output voltage at atmospheric pressure, when the heat transfer through the gas is dominant. As the gauge output voltage is proportional to the temperature difference ΔT between the heater and the environment, and ΔT is inversely proportional to the heat exchange coefficient ξ, then the heat transfer through the gas at atmospheric pressure is ca. 10 times larger than that through the membrane. The measurements can be performed at atmospheric pressure as well as at pressures in the range 10–10^5 Pa, where the air thermal conductivity is still relatively large or at lower pressures if necessary.

The expected coefficient ξ can be estimated as follows. Assume that the radius r_0 of the effectively heated area of the membrane is ca. 50 μm and the gas thermal conductivity λ_g is ca. 0.03 W/K m [18]. The distances from the heated area to the holder, L_h ca. 1 mm, and to the thermostat, L_{th} ca. 10 mm, are much larger then r_0. Thus, the heat flux from the heated area to the gas can be estimated as $P_g \sim 4\pi r^2 \lambda_g \, dT(r)/dr$ at $r \sim r_0$, where the temperature in the gas around the heater $T(r) \sim \Delta T \, r_0/r$ at L_{th} and $L_h \gg r \gg r_0$. Then $P_g \sim 4\pi r_0 \lambda_g \Delta T$ and $\xi \sim 4\pi r_0 \lambda_g$, i.e. ξ is ca. 2×10^{-5} W/K.

In fact, the measured coefficient ξ was ca. 2×10^{-5} W/K. Then, the expected maximal cooling rate $(dT/dt)_{max}$ of a sample of about 100 ng, with heat capacity C ca. 100 nJ/K, can be estimated as follows: $(dT/dt)_{max} = \Delta T \, \xi/C$. Thus, $(dT/dt)_{max}$ equals ca. 5×10^4 K/s at $\Delta T = 500$ K. The same value for the maximal cooling rate at free cooling after abrupt switching of the heating power is observed in our experiments with the empty cell and with the cell loaded with a polyethylene sample ca. 40 ng. The maximal cooling rate can be enlarged by a factor of ca. 6, if helium gas will be used. In fact, a fast cooling with a liner change of temperature with time is only possible, when the scanning rate is several times smaller than $(dT/dt)_{max}$. On the other hand, the sample's thickness d must be small enough to avoid a large temperature gradient in the sample. The temperature difference δT across a plate-like sample can be estimated as follows: $\delta T = (dT/dt)(d^2 \rho c/\lambda)$, where ρ, c and λ are the density, the specific heat capacity and the thermal conductivity of the sample, respectively. Thus, δT equals ca. 5 K at $d = 10$ μm and $dT/dt = 5 \times 10^3$ K/s for a typical polymer with $\rho c = 2 \times 10^6$ J/K m^3 and $\lambda = 0.2$ W/K m. The temperature gradient exists in the lateral direction of the membrane. Thus the sample should be placed just on the heater. Otherwise, there will be temperature gradient on the periphery of the sample outside the heater.

The thermopile measures the temperature at the membrane near the heater. In general, the thermal contact between the heater and a thin sample is sufficiently good because of adhesive forces. Nevertheless, the measured temperature does not represent the temperature of the heater/sample interface. Thus the measured temperature has to be calibrated, as described later. The heat capacities and thermal resistances of the film-heater and of the thermopile are negligibly small. The main heat capacity of the cell is therefore the effective heat capacity of the heated part of the membrane, which is ca. 2×10^{-7} J/K at room temperature. Thus the system can be described by the following parameters: the coefficient of the heat exchange, ξ, between the central part of the cell and the environment, the effective heat capacity of the central part of the cell C_0 and the heat capacity of the sample C.

The resistive film-heater, ca. 600 Ω, provides the heat flow $P_0(t)$, which is supplied to the membrane/sample interface and propagates through the

sample, membrane and the ambient gas. The equation of the heat balance is as follows:

$$(C + C_0)\frac{dT}{dt} = P_0 - \xi(T(t) - T_0), \quad (1)$$

where $T(t)$ and T_0 are the temperatures of the heating region and of the environment (of the holder in fact). This equation is correct, provided the thermal thickness of the sample is small enough and the heat transfer from the cell to the thermostat can be described by Newton's law. As it is shown later, the temperature measured by the thermopile is ca. 10 ms delayed with respect to the heater current. Therefore, the scanning rate must be less than $\Delta T/\tau_0$, where $\tau_0 = 10$ ms, i.e. smaller than 5×10^4 K/s at $\Delta T = 500$ K. This limitation is of the same order of magnitude as the restriction, which follows from the limited heat exchange through the gas. In the present work the scanning rate was less than or equal to 5×10^3 K/s, i.e. the rate was at least 10 times smaller than the limit of 5×10^4 K/s. In this case, the cooling rate can be controlled.

The heat flow $P_0(t)$ is determined by the electric current in the heater, $I_H(t)$, and its resistance $R_H(T)$. The resistance $R_H(T)$ was calibrated in advance. It changed from 475 Ω at 100 K to 706 Ω at 500 K. The electric current in the heater was monitored in real time during its scanning simultaneously with the temperature difference $T(t) - T_0$, measured by the thermopile. The temperature dependence of the thermopile sensitivity, S, was calibrated. Starting from different temperatures T_0 the temperature of the melting peak of PCL was measured at constant heating rate of 10^3 K/s and it was used as a reference temperature. A broad maximum of thermopile sensitivity around 200 K was observed. The thermopile sensitivity, ca. 1 mV/K at the maximum, changes for about 20% in the temperature range 100–500 K. Next, the thermopile thermal lag was calibrated from heating scans at different rates assuming constant melting temperature of the PCL. The shift factor was estimated as −4.1 K per 10^3 K/s. Next, these results were proved with an indium sample, for which melting temperature was assumed as independent on scanning rate.

Thus, there are three unknown parameters, ξ, C_0 and C, in Eq. (1). The parameter C_0 was determined in advance for the empty cell. The parameters ξ and C can be determined simultaneously at heating–cooling scanning. The scanning program can be repeated for monitoring a reproducible thermal process or to follow changes in time. As follows from Eq. (1), $P_0(t)$ equals $\xi[T(t) - T_0]$ at all times, when the derivative dT/dt equals zero. At repeating scanning, we have a number of successive moments t_i, when the temperature $T(t)$ is not changed. Thus, the parameter ξ can be accurately determined as the average value of ξ_i, where $\xi_i = P_0(t_i)/[T(t_i) - T_0]$ at $dT(t_i)/dt = 0$. Next, the heat capacity of the sample can be obtained according to Eq. (1) for other moments t, at which the derivative dT/dt is not zero:

$$C(t) = \frac{P_0 - \xi(T - T_0)}{dT/dt} - C_0. \quad (2)$$

In a narrow temperature range, ca. 50 K, the parameter ξ can be approximated by an average value. On the other hand, as the air thermal conductivity depends on temperature [18], the heat exchange coefficient is also a temperature dependent function $\xi(T)$. The dependence $\xi(T)$ was approximated by a smooth polynomial function, when wider scans, ca. 500 K, were studied.

3. Experimental: results and discussion

The method was applied to study melting and crystallization of the linear polyethylene standard reference material (SRM) sample NBS SRM 1484. This polyethylene has the number-average molecular weight M_n ca. 100,500 g/mol and the weight-average molecular weight M_w ca. 119,600 g/mol with the ratio M_w/M_n ca. 1.2. The crystallinity of such polyethylene is ca. 60% at room temperature [19]. The specific heat capacity of the crystalline material equals ca. 22.4 J/K mol, i.e. $c = 1.6$ J/K g, and of the amorphous material ca. 30.9 J/K mol, i.e. $c = 2.21$ J/K g, at 300 K [19]. The equilibrium melting temperature, T_m, and the heat of fusion, H_f, are equal to 415 K and 4110 J/mol, i.e. 293 J/g, respectively [20].

For studies of fast melting and crystallization the sample must be small enough and the sample should stay at the heater during thermal cycling, so the adhesion between the sample and the cell should be sufficiently good. Preliminary experiments with a paraffin and glycerol showed that at high scanning rates the sample was repelled from the heater and spread around it. This problem was not observed for high molecular weight polymers. The linear

polyethylene SRM 1484 sample ca. 10^{-7} cm^3, i.e. ca. 10^{-7} g, was placed in the cell center just at the heater. The small piece of sample was moved under a microscope to the right position by means of a hair. When the right position was reached the sample was melted by switching on the current through the heater. The sample was plate-like after melting. The volume of the sample ca. 100 μm × 100 μm × 10 μm was estimated from microscopic pictures under different view angles. This is in agreement with the results from heat capacity measurements which yield ca. 120 ng, as shown later.

The heat capacity at fast scanning was measured as described in the previous section. First, the empty cell was studied. The current in the heater (in fact the voltage at the reference resistor) and the signal from the thermopile were monitored in real time during fast scanning of the membrane temperature. The digital lock-in amplifier, EG&G Instruments 7265, was used for pre-amplification of the thermopile signal. The broad-band input amplifier of this lock-in amplifier was operating in dc-coupling mode. The auxiliary analog-to-digital converters (ADC) of the lock-in amplifier were used for converting the signals to digital information. The ADCs were running at different rates, so the time/point interval was controlled from a PC in the range 0.1–2 ms depending on the scanning time, the resolution was 1 mV in the range ± 10 V. This yield an error of about 2% for the power measurement and about 50 mK resolution in temperature for 500 K scans. To simplify the analysis of the time dependences $T(t)$ and dT/dt we tried to scan temperature almost linearly with time. A function generator, Stanford Research Systems DS340, was utilized to realize approximately constant scanning rate. The generator output voltage supplied to the heater was proportional to the square root of time.

Time dependence of the current in the heater was measured and it is shown in Fig. 2. The current through the heater yields a heat flow between zero and 10 mW. One heating–cooling cycle took 0.5 s only and was continuously repeated. The temperature of the thermostat was stabilized at 100 K. The time dependence of the electric current through the heater and that of the temperature measured by the thermopile for the empty cell are shown in Fig. 2A. The temperature was scanned almost linearly with time in the range 100–550 K. The temperature was ca. 10 ms delayed with respect to the current as shown in the insert. This delay occurs because the thermopile hot junction is placed at some distance from the heater. It yields a limitation, ca. 5×10^4 K/s, for the maximal scanning rate at $\Delta T = 500$ K.

The time dependence of the scanning rate of the cell's central part is shown in Fig. 2B. The dependence of the scanning rate versus temperature is shown in the insert. As the temperature was scanned in the broad range, 100–550 K, the membrane heat capacity $C_0(T)$ and the heater resistance were significantly changed. The increase of the heat capacity $C_0(T)$ and of the resistance $R_H(T)$ leads to the decrease of the scanning rate at high temperatures and to the enhancement of the rate at low temperatures. The time dependence of the electric current in the heater, $I_H(t)$, can be adequately adjusted, if necessary, to keep the scanning rate at a constant value. The empty cell heat capacity, $C_0(T)$, was obtained according to Eq. (1) at zero C from the curves shown in Fig. 2 in the temperature range 150–500 K. The heat capacity equals ca. 2×10^{-7} J/K at 300 K.

Then the PE sample was placed at the heater of the cell. First, in order to check stability of the sample on the sensor the sample was studied in the regime of the common temperature-modulation technique, see [15,16] for details. The oscillating heat flow was supplied to the sample from the film-heater and the temperature oscillations at the thermopile were measured by the lock-in amplifier, EG&G Instruments 7265. The measurements were performed at the heat-flow amplitude ca. 0.03 mW and at the modulation frequency $f = 5$ Hz. The amplitude of the temperature modulation was ca. 0.5 K. The thermostat temperature was scanned at a rate of ±5 K/min between 300 and 400 K. After the first heating–cooling cycle the results were reproducible. The well-defined melting and crystallization maxima of the sample's heat capacity were observed.

Next, the sample was investigated at fast heating–cooling scanning. To vary the heating and cooling rate the generator output voltage-time profile was accordingly adjusted. The well-defined changes of the scanning rate due to the sample's melting and crystallization are shown in Fig. 3.

The heat capacity $C(T)$ of the sample was calculated according to Eq. (2) from the measured time dependences $P_0(t)$ and $T(t)$, as described earlier. The

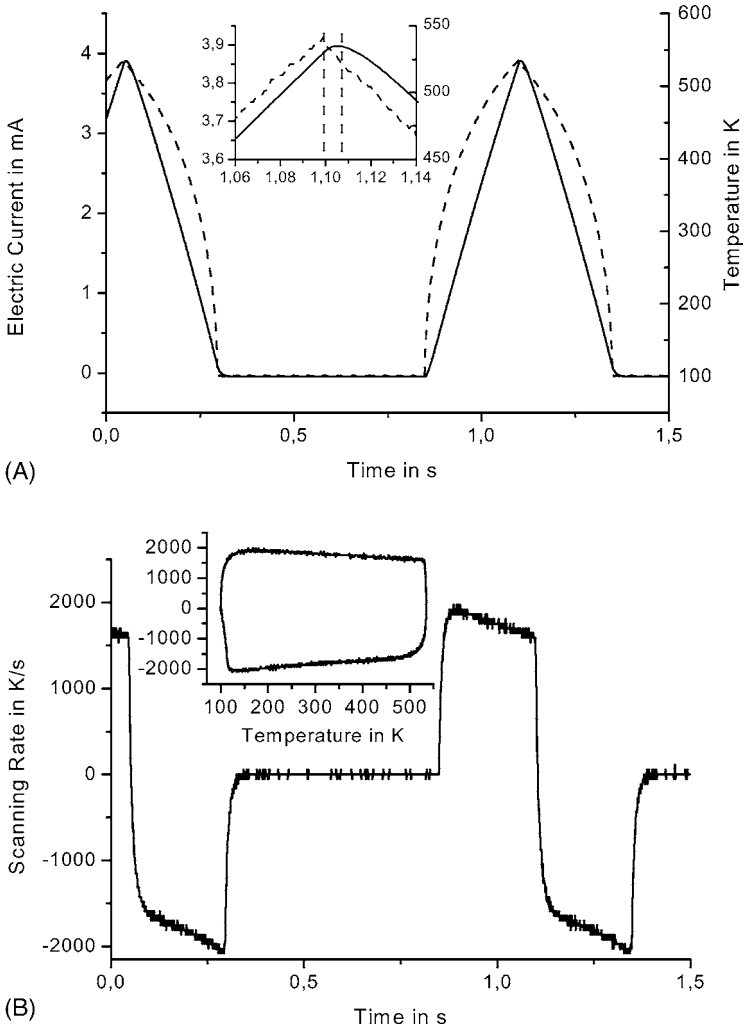

Fig. 2. (A) Time dependence of the electric current in the cell heater (- - -) and that of the temperature measured by the thermopile (—) for the empty cell. The temperature is ca. 10 ms delayed with respect to the current as shown in the insert. (B) Time dependence of the scanning rate. The dependence of the scanning rate vs. temperature is shown in the insert. The temperature of the thermostat was stabilized at 100 K.

measurements were performed at different scanning rates in the range 10^2–5×10^3 K/s. The temperature difference δT across the sample of thickness ca. 10 μm can be estimated according to the relation $\delta T = (\mathrm{d}T/\mathrm{d}t)(d^2\rho c/\lambda)$, as described earlier. The value δT was relatively small, ca. 10 K, at the largest scanning rate ca. 5×10^3 K/s. Nevertheless, some smearing of the melting and crystallization maxima of $C(T)$ dependences can be attributed to the thermal gradients in the sample and to the lag of the temperature measured by the thermopile. The dependences $C(T)$ for the crystallization and the melting process are shown in Fig. 4. The crystallization and the melting maxima of $C(T)$ dependences were smeared and shifted to lower and higher temperatures, respectively, at increasing scanning rate, as shown in Fig. 4. The positions of the maximum of the melting and crystallization peaks, measured for the same PE NBS SRM 1484 sample by a Perkin-Elmer Pyris 1 DSC at 10 K/min (0.17 K/s), are indicated in Fig. 4 too.

At cooling the well-pronounced shift of the crystallization peak to lower temperatures with increasing

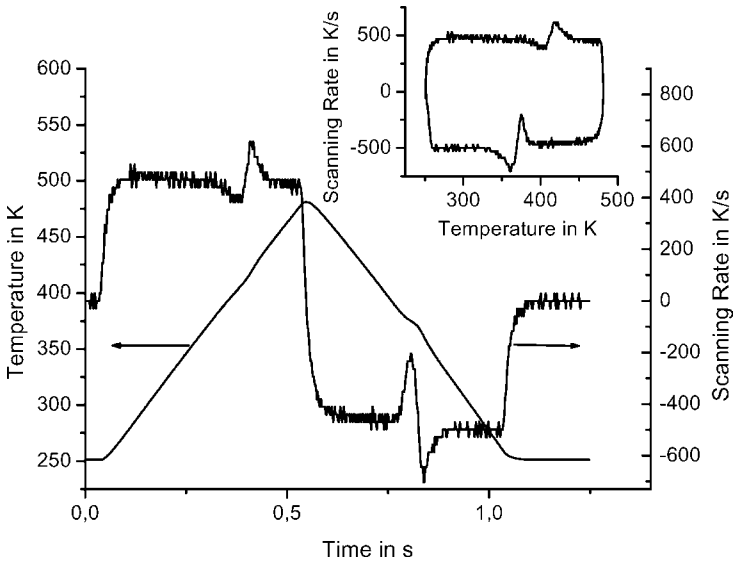

Fig. 3. Time dependences of the temperature $T(t)$ and the scanning rate dT/dt of the central part of the cell loaded by the linear polyethylene NBS SRM 1484 sample of mass ca. 120 ng. The dependence of the scanning rate vs. temperature is shown in the insert. The temperature of the thermostat was stabilized at 250 K.

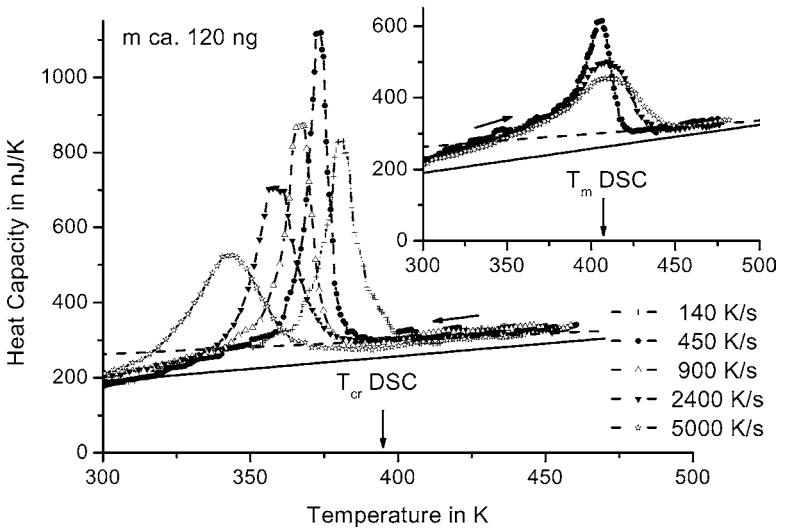

Fig. 4. Temperature dependences of the heat capacity C of the linear polyethylene NBS SRM 1484, ca. 120 ng, at crystallization at different cooling rates. The temperature dependences of the heat capacity C at melting are shown in the insert. The positions of the maximum of the melting and crystallization peaks, measured by a Perkin-Elmer Pyris 1 DSC at 10 K/min, are indicated by the arrows. The expected temperature dependences of the heat capacity of a 120 ng PE sample in amorphous and crystalline state according to [20] are shown by dashed and solid lines, respectively.

cooling rate is observed. Simultaneously the curves are more smeared as expected. The low peak height at the lowest cooling rate is caused by limitations in the resolution of the used electronics. To obtain better results at low scanning rates sample mass should be enlarged in order to get stronger signals or high sensitive analog to digital converters should be used.

DSC measurements at rates between 1 and 100 K/min show that the melting temperature T_m of this polyethylene sample stays at the same position, ca. 406.5 K, whereas the peak of the crystallization process is shifted to lower temperatures from 395 to 388 K at increasing cooling rate from 1 to 50 K/min. The heat of fusion, measured as the area under the melting peak, was ca. 166.5 J/g.

The mass of the small sample on the thin film sensor was unknown. Therefore, the sample mass was estimated from the measured heat capacity in the melt above 450 K. Using the heat capacity data from ATHAS data bank [20] we obtain a sample mass of ca. 120 ng in agreement with the size of the sample ca. 100 μm × 100 μm × 10 μm. The area under the melting peak was ca. 14,000 ± 700 nJ at different scanning rates, which corresponds to the heat of fusion ca. 120 ± 6 J/g. This is about 30% smaller than the expected 160 J/g. The area under the peak of crystallization was ca. 11,000 ± 600 nJ at different scanning rates, which corresponds to the heat of fusion ca. 92 ± 5 J/g. The given uncertainties present differences in the area between scans with different rates rather than the absolute error. At fast scanning the area under the peaks is smaller than expected, indicating some problems in calibration or that the model is too simple.

4. Conclusions

Heat capacity measurements at fast cooling and heating were realized with a thin film microcalorimeter. Crystallization and melting of a linear polyethylene NBS SRM 1484 sample of mass ca. 120 ng was studied. Relatively high cooling rates, ca. 5×10^3 K/s, were achieved. The measurements were performed in an ambient gas. The conditions were nonadiabatic, but the heat leakage from the sample could be calibrated. It was shown that the described simple calibration algorithm can be used for heat capacity measurements. In this first approximation uncertainty was about 30% for heat of fusion.

Almost constant cooling–heating rates, up to $\pm 10^3$ K/s, were realized when a certain input function is used for the power applied to the heater by means of a function generator. To study melting and crystallization at these rates one needs small and thin samples, ca. 100 ng and ca. 10 μm. For polyethylene the melting temperature is only little dependent on heating rate but crystallization temperature shows the expected cooling rate dependency. For linear polyethylene a cooling rate of 5×10^3 K/s is not high enough to prevent crystallization. For other fast crystallizing materials like polyethylenoxide (PEO) and ε-polycaprolactone (PCL) it was possible to produce amorphous samples at such rates [21].

The calibration, especially of thermopile sensitivity, has to be improved to obtain more precise data on heat capacity and heat of fusion. To avoid most of the calibration problems, which are due to the finite distance between heater and thermometer, a cell with the heater and the thermometer at the same place (layered system) may be preferable.

Acknowledgements

We acknowledge fruitful and stimulating discussions with M. Merzlyakov who advised us to try the vacuum gauge as a calorimetric sensor for this study. The financial support of the German Science Foundation (DFG), grant numbers SCHI 331/7 and 436 RUS 17/108/01 is gratefully acknowledged.

References

[1] T.F.J. Pijpers, V.B.F. Mathot, B. Goderis, R.L. Scherrenberg, E.W. van der Vegte, Macromolecules 35 (2002) 3601.
[2] V. Brucato, F.G. Crippa, S. Piccarolo, G. Titomanlio, Polym. Eng. Sci. 31 (1991) 1411.
[3] Z. Ding, J.E. Spruiell, J. Polym. Sci.: Part B: Polym. Phys. 34 (1996) 2783.
[4] V. Brucato, F. De Santis, A. Giannattasio, G. Lamberti, G. Titomanlio, Macromol. Symp. 185 (2002) 181.
[5] M. Zhang, M.Y. Efremov, F. Schiettekatte, E.A. Olson, A.T. Kwan, S.L. Lai, T. Wisleder, J.E. Greene, L.H. Allen, Phys. Rev. B 62 (2000) 10548.
[6] M. Zhang, M.Y. Efremov, E.A. Olson, Z.S. Zhang, L.H. Allen, Appl. Phys. Lett. 81 (2002) 3801.

[7] S.L. Lai, G. Ramanath, L.H. Allen, P. Infante, Appl. Phys. Lett. 70 (1997) 43.
[8] A.T. Kwan, M.Y. Efremov, E.A. Olson, F. Schiettekatte, M. Zhang, P.H. Geil, L.H. Allen, J. Polym. Sci. B: Polym. Phys. 39 (2001) 1237.
[9] J. Bennett, Proc. NATAS 2002 (2002) 150.
[10] T.W. Kenny, P.L. Richards, Phys. Rev. Lett. 64 (1990) 2386.
[11] D.W. Denlinger, E.N. Abarra, K. Allen, P.W. Rooney, M.T. Messer, S.K. Watson, F. Hellman, Rev. Sci. Instrum. 65 (1994) 946.
[12] N.E. Hager, Rev. Sci. Instrum. 35 (1964) 618.
[13] L.H. Allen, private communications.
[14] B. Frochte, Y. Khan, E. Kneller, Rev. Sci. Instrum. 61 (1990) 1954.
[15] M. Merzlyakov, C. Schick, Proc. NATAS 2000 (2000) 714.
[16] M. Merzlyakov, Thermochim. Acta (2003), this issue.
[17] Technical data available on the website: http://www.xensor.nl/pdffiles/tcg3880.pdf.
[18] D.R. Lide (Ed.), Handbook of Chemistry and Physics, 79th ed., CRC Press, 1999, pp. 6–175; or on the website: http://users.wpi.edu/∼ierardi/PDF/air_k_plot.PDF.
[19] V.B.F. Mathot, M.F.J. Pijpers, J. Thermal Anal. 28 (1983) 349.
[20] Athas databank: http://web.utk.edu/∼athas/.
[21] S. Adamovsky, submitted for publication.